Nature Environment and Pollution Technology
An International Quarterly Scientific Journal

p-ISSN: 0972-6268
e-ISSN: 2395-3454

Vol. 18 | No. 2 | pp. 459-469 | 2019

Original Research Paper | Open Access

Hotspots Identification of Heavy Metals in Sediments and Revelation of the Relationship Between Heavy Metal Contents and Environmental Variables

Aijun Peng and Wen Wang†
Center for Spatial Information, School of Environment and Natural Resource, Renmin University of China, Beijing 10082, China
†Corresponding author: Wen Wang

Nat. Env. & Poll. Tech.
Website: www.neptjournal.com

Received: 10-06-2018
Accepted: 21-09-2018

Key Words:
Spatial autocorrelation
Metal hotspots
Sediments
Spatial regression analysis
Heavy metals

ABSTRACT

The aim of the study was to identify the hotspots of heavy metals in sediments for exploring possible sources and understand the relationship between heavy metals and environmental variables. West Chaohu Lake was selected as the study area, 38 surface sediment samples and 4 river mouth sediment samples were obtained and analysed for three typical metals (i.e. Co, Mn and Pb). Local indicators spatial associate (LISA) analysis detected spatial clusters and spatial outliers of enrichment factor (EF) values of the three metals and found the samples with pollution belong to high-high clusters, low-low clusters, even low-high outliers. Geostatistics and local Moran's I were combined, and the results indicated that Co is mainly from natural sources, Mn is influenced by upward migration and reprecipitation, and Pb is influenced by anthropogenic sources. Furthermore, Pb was chosen as an example to understand the relationship between heavy metals and environmental variables. Compared to ordinary least squares (OLS) model, spatial autoregressive regression (SAR) model performed better and accounted for the phenomenon of spatial autocorrelation. Grain particle percent, loss on ignition (LOI), distance to Nanfei River mouth has a significant influence on the variation of Pb concentrations in sediments. Hotspots identification and spatial regression analysis can play an important role in understanding the pollution process for pollution management and restoration.

INTRODUCTION

Heavy metals are non-biodegradable and can pose a large ecological risk, so their pollution has been an environmental issue of public concern (Wang et al. 2012). When entering aquatic systems, heavy metals in water column would ultimately accumulate in sediments (Dassenakis et al. 2003). If the physico-chemical conditions of the water-sediment interface were changed, heavy metals may be desorbed from sediments, and then threaten food chains and the ecosystems, ultimately endangering human health (Hu et al. 2014, Senesi et al. 1999). So, it is very important to identify hotspots and reveal the relationship between heavy metals and environmental variables for pollution control and policy making.

Previous studies have usually employed contour to identify hotspots of heavy metals, e.g. Yuan et al. (2014) found some metals had two hotspots with high concentrations in soils of typical urban renewal area in Beijing, China. Nevertheless, the hotspots identification based on the contour is influenced by many factors, such as the number of levels and the range of each level. Furthermore, the significance of hotspots identified by contour cannot be tested. Fortunately, there exists another method, spatial autocorrelation analysis method, which also can be implied to identify hotspots of pollutants and to test the significance of hotspots.

Liu et al. (2013) and Huo et al. (2011) have implied local Moran's I, a kind of spatial autocorrelation analysis method, to identify hotspots of pollutants resulting from anthropogenic sources in soils. However, different from soils, hotspots of pollutants in sediments can be caused by upward migrations and reprecipitation due to geochemical characteristics in addition to anthropogenic sources (Yuan et al. 2012). Due to the complexity of pollutant sources in sediments, the feasibility of local Moran's I in the exploration of possible sources of pollutants in sediments was unknown.

For metals influenced by anthropogenic sources, it is important to measure the relationship between their concentrations and the influencing environmental variables for better understanding the pollution process. There have been only a few studies that explored the relationship. In this study, spatial autoregressive regression (SAR) model was employed to understand the relationship, which accounts for spatial autocorrelation phenomenon, i.e., that values close together in space are generally more similar than values located farther apart. SAR model has been popularly

used in many aspects, including homicide patterns (Ye & Wu 2011), invasive alien plants (Dark 2004) and land use (Overmars et al. 2003).

In this paper, West Chaohu Lake was selected as the study area. Previous studies have found that Co in sediments of Chaohu Lake is mainly from natural sources, Mn might be affected by upward migrations, and Pb is influenced by anthropogenic sources (Liu et al. 2012b, Zheng et al. 2011). The three metals were focused in this study. Moran's I, SAR model, enrichment factor (EF) and geographic information system (GIS) were combined. The purpose was to: 1. test whether exploration of the possible sources of Co, Mn and Pb based on local Moran's I is feasible or not; 2. reveal the relationship between heavy metal concentrations and environmental variables.

MATERIALS AND METHODS

Study area: Chaohu lake, one of the five largest freshwater lakes in China, lies within 117°16'54"-117°51'46" E and 31°25'28"-31°43'28" N, and is located in the middle-lower reaches of Yangtze River watershed and central Anhui Province. Chao Lake has an average depth of 2.7 m, with a water surface area of about 770 km^2 and a watershed area of 13,350 km^2. The watershed of this lake has an annual mean temperature of 16°C and an annual mean rainfall of 996 mm with a subtropical monsoon climate. The lake has 33 inflow rivers, of which Hangbu River, Nanfei River and Baishishan River are the three largest rivers, accounting 85.4% of the annual runoff. There is only one outflow river (Yuxi River), which is located east of the lake and feeds the Yangtze River.

In the last 3 decades, Chaohu Lake has witnessed significant economic growth and urban development in its watershed. Meanwhile, this lake, especially west Chaohu Lake, has experienced serious pollution, because of the discharge of massive industrial and domestic sewage (Liu et al. 2012b). For example, in 1997, the discharge of sewage into this lake was estimated to about 1.9×10^8 tons, 80% of which was from Hefei City, the biggest city in the watershed (Dang 1998). The pollution of Nanfei River, the main sewage discharge channel for Hefei city and Feidong county, is more serious than that of other rivers.

Sediment sampling and analysis: Thirty-eight and four surface (0-2 cm) sediment samples were obtained from the west Chaohu Lake and at the river mouth, respectively, using a gravity corer with latitudes and longitudes positioned using Global Positioning System (GPS) in April 2016. Sampling sites are depicted in Fig. 1. The samples were transferred into plastic bags and placed in an icebox temporarily. After transported to the laboratory, these sediments were stored at 4°C.

Sediments were freeze-dried and ground with agate mortar, and then totally digested with HCl-HNO_3-HF-$HClO_4$. Metal concentrations were determined by the inductively coupled plasma-atomic emission spectrometry (ICP-AES). The accuracy and precision of the experiment were ensured using blanks, replicates and standard reference sediments offered by the Chinese Academy of Geological Sciences, throughout the analysis. Grain size distribution of sediment

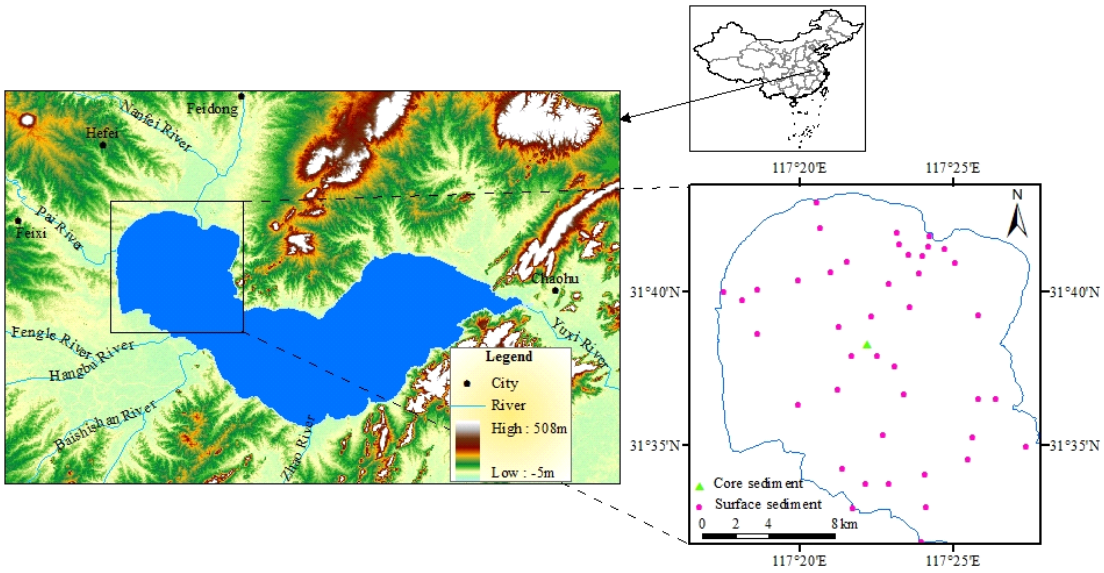

Fig. 1: Study area and distribution of sampling sites.

samples was determined by a Malvern Mastersizer 2000 after removing of organic matter with 20% HCl, washing, and ultrasonic dispersion. The organic matter content was determined as a loss on ignition (LOI) following 4-h ignition (550°C).

Enrichment factor: Metal concentrations in sediment were influenced by grain size effects, which may complicate the pollution determination only based on the concentrations. Enrichment factor (EF), an effective method for reducing these effects, can be employed (Wang et al. 2015) and the EF value reflects the environment pollution status. The equation of EF can be written as follow:

$$EF = (M_{sample}/N_{smaple})/(M_{background}/N_{background}) \quad ...(1)$$

Where, M_{sample} is the concentration of evaluated metal in interested sediments, N_{smaple} is the concentration of normalizing metal in interested sediments, $M_{background}$ is reference concentration of the evaluated metal, $N_{background}$ is the reference concentration of the normalizing metal. EF < 2 represents deficiency to minimal metal pollution, and EF > 2 indicates various degrees of metal pollution (Han et al. 2006).

Selecting an appropriate normalizing metal and establishing the reference concentrations are important issues in EF calculation. Due to the inertness in migration process and originating mainly from natural lithogenic sources, Al is usually used as the normalizing metal (Wang et al. 2015). Compared with metal concentrations in average crustal abundances, metal concentrations in pre-industrial sediments are considered more suitable to be used as reference background (Liu et al. 2012a).

Local Moran's I: Spatial autocorrelation can be used to assess the correlation of a variable related to its position, which measures the matching between position similarity and value similarity (Huo et al. 2012). Moran's I is a widely used method for spatial autocorrelation. Local Moran's I index is a local index for spatial correlation, and can be employed for identifying the locations of spatial clusters and spatial outliers. Local Moran's I can be computed as follows:

$$I_i = \frac{n(x_i - \bar{x}) \sum_{j=1, j\neq i}^{n} w_{ij}(x_j - \bar{x})}{\sum_{i=1}^{n}(x_i - \bar{x})^2} \quad ...(2)$$

Where, n is the number of observed locations in the whole region, x_i and x_j are values of the selected variable at locations of i and j, $\bar{x}$ is the average value of x, w is the spatial weights matrix, and w_{ij} is the spatial weight between locations i and j.

The weights matrix describes the spatial relationship between each location and its nearby locations. Generally, the weights are on the basis of contiguity relations or distances. In this paper, a distance-based weight matrix was employed, and a given distance is selected in order to judge whether the distance between location i and location j is within the given distance or not. If within, the location i is regarded as a neighbour of location j, and the corresponding weight is assigned with 1. If not, the weight is assigned with 0.

After the calculation of local Moran's I, five kinds of local spatial autocorrelation could be identified. Two of these belong to spatial clusters, including high-high (high values having high-value neighbours) and low-low (low values having low-value neighbours) clusters. Two belong to spatial outliers, including high-low (high values having low value neighbours) and low-high (low values having high neighbours) outliers. The last kind represents insignificant spatial autocorrelation, which indicates spatial randomness. In general, high-high spatial clusters are "regional hotspots", low-low spatial clusters can be regarded as "cool spot" indicating that there was no pollution, and high-low spatial outliers can be viewed as isolated "individual hotspots", implying the existence of point source pollution.

Geostatistical analysis: Geostatistics employed semivariogram to represent spatial variability of regionalized variable and to provide the input parameters for kriging (Huo et al. 2012). The semivariogram can be calculated as the following formula:

$$\gamma(h) = \frac{1}{2N(h)} \sum_{i=1}^{N(h)} [Z(x_i + h) - Z(x_i)]^2 \quad ...(3)$$

Where, $\gamma(h)$ expresses the semivariance value for observed pairs at a lag distance h, $N(h)$ states the number of observed pairs of sampling sites separated by the distance h, $Z(x_i)$ is the value of the regionalized variable Z at the site x_i, $Z(x_i+h)$ is the value of the regionalized variable Z at the site x_i+h.

Geostatistics has 11 different theoretical semivariogram models, such as Gaussian model and Stable model. Among these models, the best-fit one for current semivariogram can be selected by the highest coefficient value. Once the best-fit model is selected, several parameters, including range, sill, and nugget can be obtained and taken as the input parameters for kriging interpolation.

Kriging is regarded as an optimal interpolation technique owing to unbiased estimation and has lots of variants. Among these variants, ordinary kriging (OK) is the most frequently-used interpolation methods for mapping the spatial pattern of heavy metals. So, in this study, OK

was employed to generate the spatial distributions map for EF values of heavy metals.

Spatial regression analysis: SAR model that is devised to account for the phenomenon of spatial autocorrelation was carried out to quantify the relationship between heavy metal concentrations in sediments and the influencing factors. Compared to OLS model, SAR model complements a term that incorporates the spatial autocorrelation structure of a given data set. The term is implemented with a spatial weight matrix, where the neighbourhood weight of each location can be defined by contiguity relations or distances (Zhang et al. 2011). In this study, the spatial weight matrix is the same as the spatial weight matrix used in Local Moran's I. SAR method has two basic models (spatial lag model and spatial error model), distinguished by where the spatial autoregressive process is believed to occur (Zhang et al. 2011).

Spatial lag model assumes that the spatial autoregressive process can be only discovered in the dependent variable (Kissling & Carl 2008). Hence, the spatial lag model implies that pollutant concentrations at each location are jointly determined by pollutant concentrations observed at nearby locations and a set of local independent variables (Meyfroidt & Lambin 2008, Ye & Wu 2011). The equation of the spatial lag model is written as follow:

$$y = \rho Wy + X\beta + \varepsilon,\ \varepsilon \sim N(0,\sigma^2) \quad ...(4)$$

Where, y is a (n×1) vector of observations on the dependent variable, X is a (n×k) matrix of observations on the independent variables, ρ is a coefficient on the spatially lagged dependent variable, w is a known (n×n) spatial weights matrix, β is a (k×1) vector of fixed but unknown parameters, and ε is a (n×1) vector of errors assumed to be independent identically normally distributed.

Spatial error model assumes that the spatial autoregressive process only exists in the error term (Kissling & Carl 2008). Hence, spatial error model indicates that pollutant concentration at each location depends on a set of observed local indicators and that the error term is spatially autocorrelated (Meyfroidt & Lambin 2008,Ye & Wu 2011). The equation of spatial error model is expressed as follow:

$$y = X\beta + \lambda Wu + \varepsilon, \varepsilon \sim N(0,\sigma^2) \quad ...(5)$$

Where, λ is a coefficient on the spatially correlated errors, u is a (n×1) vector of spatial autocorrelated errors, and the rest notions are as above.

In short, spatial lag model is consistent with the situation where pollutant concentration is jointly determined with that of nearby locations, while spatial error model is consistent with a situation where determinants of pollutant concentrations omitted from the model are correlated over space, and with a situation where unobserved factors follow a spatial pattern (Su et al. 2011, Ye & Wu 2011).

In the presence of spatial autocorrelation, the traditional OLS model is not appropriate to explore the relationship among pollution process. So, the SAR model estimated by Maximum Likelihood method is employed (Dark 2004). The selection of a goodness-of-fit spatial model is also an important affair in spatial regression analysis. In general, the Lagrange Multiplier diagnostics is employed to choose whether the spatial lag model or spatial error model is a suitable alternative to OLS model (Su et al. 2011). The tradition R^2 based on OLS model (decomposition of the total sum of squares into explained and residual sums of squares), is not applicable to quantify the goodness of spatial regression model fit (Overmars et al. 2003). Fortunately, the pseudo R^2 can be calculated. It should be noted that the traditional R^2 cannot be compared with the pseudo R^2 and the pseudo R^2 of different spatial regression models can be compared (Overmars et al. 2003). In addition, Log Likelihood (LIK), Akaike Information Criterion (AIC) and Schwartz Criterion (SC) are also measures for spatial regression model fit (Hession & Moore 2011, Wang 2007). The higher LIK or the lower AIC or SC, the better the model is fit.

Data analysis: The basic statistical parameters were calculated using SPSS 19.0, Local Moran's I and SAR model were implemented using OpenGeoDa 1.2.0, while OLS model was estimated using both SPSS 19.0 and OpenGeoDa 1.2.0, geostatistical analysis, and spatial distribution maps of metals were performed with ArcGIS 10.3.

RESULTS AND DISCUSSION

Descriptive statistics: Descriptive statistics of metal concentrations and the EF values, including mean, skewness, and kurtosis, are given in Table 1. The concentration ranges of Al, Co, Mn and Pb were 32.89-92.50 g/kg, 7.77-21.01 mg/kg, 314.33-1824.60 mg/kg and 17.93-100.85 mg/kg, respectively. Furthermore, when Al was selected as normalizing metal and metal concentrations of deep part (65-90 cm) of core sediments (Fig. 1), corresponding to the pre-industrial period with lower population and extensive agricultural activities (Chen et al. 2011), were selected as the reference concentrations, EF values for Co, Mn, and Pb were calculated, with the ranges 0.78-1.18, 0.83-2.51 and 1.05-3.89, respectively. After comparison, Mn and Pb were found to have wider ranges. In addition, Kolmogorov-Smirnov test for normality (*K-S p*) was conducted to check the normality of metals of concentrations and the EF values. Results demonstrated that the values of all metals and their EF values were more than 0.05, indicating these metals were normally distributed.

Table 1: Descriptive statistics for metals and their EF values.

	Range	Mean	SD	Skewness	Kurtosis	RC	K-S p
Al (g/kg)	32.89-92.50	69.33	16.13	-0.39	2.01	49.0	0.14
Co (mg/kg)	7.77-21.01	15.84	3.84	-0.50	2.12	12.2	0.16
Mn (mg/kg)	314.33-1824.60	1103.10	395.18	-0.15	2.07	407.6	0.88
Pb (mg/kg)	17.93-100.85	60.61	23.06	0.07	2.04	21.3	0.71
EF (Co)	0.78-1.18	0.92	0.08	1.13	5.47	-	0.19
EF (Mn)	0.83-2.51	1.88	0.36	-0.67	3.65	-	0.82
EF (Pb)	1.05-3.89	2.04	0.58	0.41	3.71	-	0.65

SD: standard deviation; RC: reference concentration.

Table 2: The value of Global Moran's I and sample distribution in local spatial patterns types.

	Types	EF(Co)	EF(Mn)	EF(Pb)
Global Moran's I	Global Moran's I	-0.13	0.49	0.65
	Standardized Global Moran's I	-1.07	5.06	6.83
Local Moran's I	No significance (%)	97.6	69.1	40.4
	High-high (%)		21.4	31.0
	Low-low (%)		9.5	26.2
	Low-high (%)			2.4
	High-low (%)	2.4		

Local indicators of spatial association (LISA): In order to understand the pollution condition for better remediation, hotspots and cool spots need to be identified. This can be achieved by local Moran's I. Because cool spots are considered to be clean, this study mainly focused on the identification of hotspots, which may be regional hotspots (spatial clusters) or individual hotspots (spatial outliers). The distance bands for EF values of Co, Mn and Pb of Local Moran's I index all were 3500 m. The spatial patterns for the three metals are exhibited in Fig. 2 and the spatial clusters and spatial outliers are significant at the 0.05 level. Nevertheless, the three metals only had one high-low outlier (Fig. 2), so only high-high clusters were focused on.

Zhang et al. (2008) employed local Moran's I and GIS to identify pollution hotspots of Pb in soils, and discovered that different distance bands generated different results. So, he recommended that many related factors should be taken into consideration when selecting appropriate distance bands. Furthermore, Huo et al. (2012) studied spatial autocorrelation characteristics based on the distance where the standardized Moran's I reached maximum. They found the results based on the former distance can detect the local highlights of local spatial pattern. So, in this study, this criterion is adopted for selecting suitable distance bands. The distance bands for EF values of Cu, Mn, Pb and Zn all were 3500 m, corresponding to each distance where the Moran's I reached maximum, respectively.

As Table 2 shows, global Moran's I of Co, Mn and Pb were 0.13, 0.49 and 0.65, respectively. Furthermore, global standardized Moran's I that was employed to test whether the spatial autocorrelation is significant or not at the global level was calculated, and the result showed that Co did not pass the significant level test (1.96). For global Moran's I and global standardized Moran's I, more details can be referred to other literature (Huo et al. 2011, Liu et al. 2013). As to local spatial pattern, less than half of the samples of all metals exhibited significant spatial patterns except Pb. In addition, because the standardized Global Moran's I was -1.07, such a large percentage of samples without significant spatial patterns can be expected. 30.9% for Mn and 57.2% for Zn samples belonged to significant spatial clusters, which dominated the whole significant spatial patterns. Low-low clusters of samples for Pb were about half of that of spatial clusters, while high-high clusters for Mn accounted for a large proportion of that of spatial clusters. 2.4% for Co and 2.4% for Pb samples belonged to the significant spatial outliers, while the former all were in low-high outliers and the latter all were in high-low outliers. These significant spatial patterns imply that there is some extent of spatial enrichment of Mn and Pb in sediments.

In addition, samples were classified based on pollution status and local spatial pattern types (Table 3). All samples were not polluted by Co. The samples with Mn pollution were 35.7% and among these, 14.3% belonged to no significant spatial pattern type and 21.4% occurred in high-high outliers. For Pb, more than half of the samples were polluted. Among these, 21.4% of samples occurred in no significant spatial pattern type, 31.0% in high-high clus-

ters, and 2.4% in low-high outliers. In short, the three typical metals had obviously different sample distributions based on pollution status and local spatial pattern.

LISA map exhibited a spatial distribution of the interesting spatial patterns for the three metals in sediments (Fig. 2). For Co, one high-low outlier was found at the mouth of Pai River. For Mn, several high-high clusters and low-low clusters were located in the central part of the study area and in the northwest part of the study area, respectively. For Pb, north part of the study area was dominated by high-high clusters, with one low-high outlier found among these, and northwest part and south part of the study area was distributed by several low-low clusters. This indicated that the three typical metals also displayed distinctly different local spatial pattern characteristics.

Spatial distribution of EF values of heavy metals: As Table 4 exhibits, the EF values of different metals had different best-fit semivariogram models whose coefficient values were highest. Semivariogram models for metals were suitable for a K-Bessel model (Co), Gaussian model (Mn) and Stable model (Pb). The ratio of nugget/sill (RNS) could be employed to assess the level of spatial dependence for metals in sediments, with RNS less than 25% implying high spatial dependence, RNS between 25% and 75% suggesting moderate spatial dependence, and RNS more than 75% indicating weak spatial dependence (Li et al. 2014). According to this criterion, Co and Mn showed high spatial dependence, with RNS of 23.1% and 23.5%, respectively, whereas, Pb showed weak spatial dependence, with RNS of 55.7%.

The distribution maps of EF values of the typical three metals are exhibited in Fig. 3. The maps show that three metals had obviously different spatial distribution patterns. For Co, its EF value changed a little in the whole study area. EF values of Mn were highest in the central part of the study area, with an increasing trend from shore to center, which contradicted the common phenomenon, i.e. that high EF values generally occur in sediments of polluted river mouth (Yin et al. 2011, Zhang et al. 2009). EF values of Pb were highest in the northeast part of the study area, the nearby region of Nanfei River mouth, exhibiting a northeast-southwest decreasing trend.

Pollution sources exploration: Domestic sewage, industrial wastewater, and agricultural effluent are main external anthropogenic sources for metals and they combined with natural sources mainly through rivers entering into the lake. It should be noted that anthropogenic sources and natural sources of metals can be distinguished by the EF value. Atmospheric deposition has been considered as a significant anthropogenic source of metals, for instance in Taihu Lake, another lake in middle-lower reaches of Yangtze River, continuous increase of atmospheric pollutant flux since 1960 was recorded in core sediments (Rose et al. 2004). In addition, the upward migration may cause an increase in the metal concentration in sediments (Anschutz et al. 2005).

Atmospheric deposition may be an important source of influencing metal concentration in sediments. The range of west Chaohu Lake was about 13 km in the east-west direction and about 18 km in the south-north direction and should be considered as a smaller region when compared with the range of atmospheric deposition. Furthermore, the elevation around Chaohu Lake is low (Fig. 1), and thus this would have little effect on atmospheric deposition. So, if atmospheric deposition contributions are significant for Pb in whole west Chaohu Lake, the EF values should be higher. However, in fact, in some areas the EF values of Pb were around 1 (Fig. 3), indicating that Pb was primarily from natural sources (Wang et al. 2015), disproving this hypothesis. The condition of Co and Mn is similar to that of Pb.

The high-high clusters of EF values of Pb (more than 2.4) mainly occurred in the area around the mouth of Nanfei River, the most polluted rivers among inflow rivers of west Chaohu Lake, as well as, the EF values of Pb decreased drastically as the distance to the mouth of Chaohu Lake increased (Fig. 3). Meanwhile, the RNS of Pb between 25% and 75% showed moderate spatial dependence exhibiting extrinsic factors (e.g. anthropogenic sources), which may weaken the dependence (Li et al. 2014). Pb concentrations in the water body of Nanfei River were relatively high (Li et al. 2011). These all indicated that high-high clusters of Pb mainly resulted from the anthropogenic sources. No high-high cluster of EF values of Mn occurred in the nearby region of the mouth of Nanfei River, while several high-high clusters of Mn occurred in the region far away from Nanfei River mouth; moreover, higher EF values mainly occurred in this region (Fig. 3), indicating that there were other factors influencing Mn. Some studies found upwards migration of dissolved Mn in sediments and reprecipitation of MnO_2 in oxic surface sediments (Anschutz et al. 2005). Therefore, high-high clusters of Mn may be induced by upwards migration and reprecipitation due to geochemical characteristics. Cobalt only had one sample in the high-low outlier, and the EF value for this sample was just 1.10, indicating that the sample was slightly influenced by anthropogenic sources. In addition, the EF values of Co in the whole study area were around 1, meaning Co is mainly from natural sources.

In LISA analysis, the typical three metals showed obviously different characteristics, including the sample distribution in local pattern types and LISA map. From the sam-

Table 3: Sample percent based on pollution status and local spatial pattern types (%).

	Pollution status	No significance	High-high	Low-low	Low-high	High-low
EF (Co)	Polluted					
	Unpolluted	97.6				2.4
EF (Mn)	Polluted	14.3	21.4			
	Unpolluted	54.8		9.5		
EF (Pb)	Polluted	21.4	31.0		2.4	
	Unpolluted	19.0		26.2		

Table 4: Best-fit semivariogram models for EF of metals and their parameters (OK).

	Model	Nugget(C_0)	Sill(C_0+C)	Range(m)	RNS(%)	R^2
EF (Co)	K-Bessel	0.0012	0.0052	18,172	23.1	0.804
EF (Mn)	Gaussian	0.0348	0.1483	6,481	23.5	0.831
EF (Pb)	Stable	0.1841	0.3304	10,231	55.7	0.813

Table 5: Global Moran's I value of different variables (based on 3500m).

	Grain Particle Percent	LOI	Distance	Pb Concentration
Global Moran's I	0.44	0.35	0.84	0.74
Global Standardized Moran's I	4.21	3.28	8.58	6.89

ple distribution in local pattern type perspective, the sample distribution of metal mainly from natural sources (Co) is different from that of metal influenced by other sources (Mn and Pb). Nearly all samples of Co belonged to no significant spatial pattern. While, Mn and Pb had several samples in high-high clusters and several low-low clusters, and may have some samples in low-high outliers. Furthermore, the samples in high-high clusters generally were polluted according to the EF values and the samples in the low-low cluster mainly were unpolluted. From LISA map perspective for metals influenced by other sources, the position of hotspots, especially regional hotspots may be different. If the high-high clusters were mainly in the region around the polluted river mouth, the metal may be influenced by anthropogenic sources (Pb in this study). If the high-high clusters were mainly in the region away from the polluted river mouth, the metal may be influenced by upwards immigration and reprecipitation (Mn in this study). So, local Moran's I can be employed to not only effectively find hotspots of metals, but also identify the pollution sources in combination with other methods.

There is an interesting phenomenon that for metals influenced by other sources (Mn and Pb), they do not have samples in high-low outliers. Tang et al. (2013) studied the clusters and outliers of heavy metals in urban street dust of Beijing and found several high-low outliers of metals resulting from point sources, such as factories and construction activities. Different from dust, metals in sediments seldom have high-low outliers. Atmospheric deposition, as the non-point source, impossibly brings about these outliers, and anthropogenic sources in general cause regional hotspots (Pb in the region around Nanfei River mouth). In addition, the upwards migration and reprecipitation rarely cause high-low outliers because the influencing factors as environmental variables are spatially dependent and scarcely change drastically.

The relationship between heavy metal concentrations and environmental variables: Herein, the relationship between concentrations of metals influenced by anthropogenic sources and environmental variables were studied, and Pb was selected as an example. As previously discussed, the influence of atmospheric deposition on metals is insignificant, so anthropogenic sources entering into the lake via rivers were focused on. In west Chaohu Lake, there are four main inflow rivers (Nanfei River, Pai River, Hanngbu-Fengle River, Baishishan River), and the EF values of Pb in corresponding river mouth sediments were 3.89, 1.07, 1.21, 1.24, respectively. So, the distance to the mouth of Nanfei River, the most polluted river, was selected as an environmental variable that influence Pb concentrations in sediments. Furthermore, the concentration of metals in sediments is influenced by other factors, mainly including grain size and organic matter content (Yuan et al. 2012). Therefore, three variables, including the distance to Nanfei River mouth,

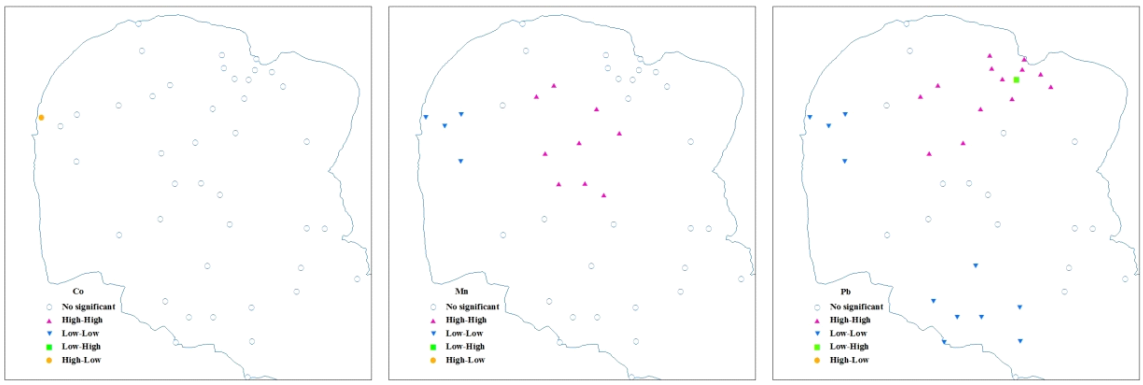

Fig. 2: LISA map for EF values of heavy metals in sediments.

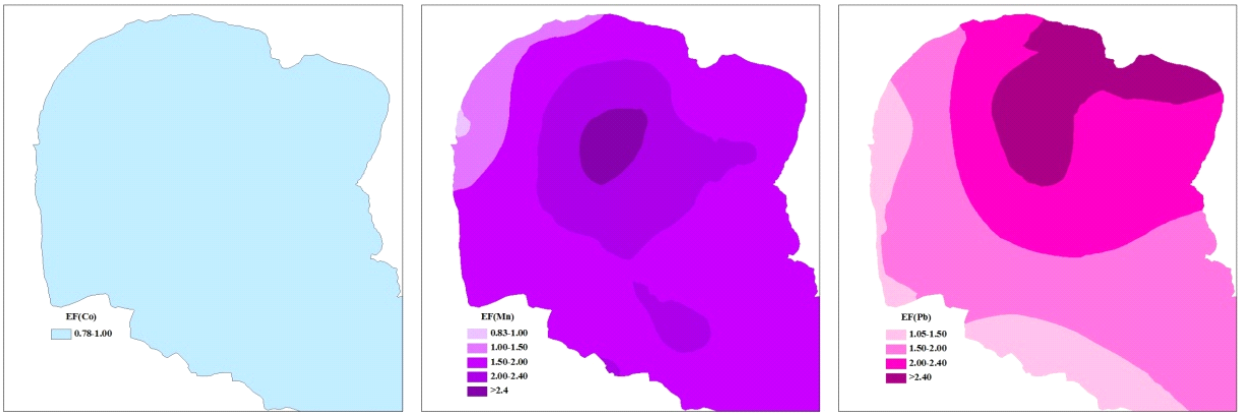

Fig. 3: Spatial distribution for EF values of heavy metals in sediments.

grain particle percent (in this paper <16 m), and organic matter content (measured as LOI) were selected as independent environmental variables. Then OLS model and SAR model were employed to explain the variation of Pb concentrations in sediments of west Chaohu Lake.

Before the spatial regression analysis, the Moran's I test was conducted for spatial autocorrelation of dependent and independent variables. The global standardized Moran's I values (based on 3500 m distance band, where the Moran's I values of all variables reached maximum) of grain particle percent, LOI, the distance to Nanfei River mouth, and concentrations of Pb in sediments were 4.21, 3.28, 8.58 and 6.89, respectively (Table 5), indicating each corresponding variable exhibited positive significant spatial autocorrelation, violating the underlying assumption of OLS model (Dark 2004).

Significant independent variable estimates and a higher R^2 (0.822) seemed that OLS model was a fit model (Table 7). Nonetheless, there was significant spatial autocorrelation for regression residuals (Moran's I = 0.148). This means that OLS model was not fit to explore the relationship between variables. So, the SAR model that accounts for spatial autocorrelation should be employed to solve this problem. Then, Lagrange Multiplier (i.e. LM, including LM-lag, Robust LM-lag, LM-error and Robust LM-error) tests were calculated to decide whether either spatial lag model or spatial error model is a suitable alternative to OLS model using OLS results and tested for significance. 5% was selected as the significance level for all diagnostic testing. As Table 6 shows, among the four diagnostic statistics, LM-error and Robust LM-error are insignificant, while the rest were significant. So, the spatial error model corresponding to Robust LM-error and LM-error was not appropriate in the spatial regression analysis, while the spatial lag model was implied to model heavy metals data.

The Moran's I value of regression residuals of the spatial lag model, 0.009, appeared to be a satisfactory result for correcting the problem of residual dependency in OLS

Table 6: LM test for SAR model.

Test	Value	Probability
LM-lag	5.800	0.016
Robust LM-lag	4.291	0.038
LM-error	1.513	0.219
Robust LM-error	0.004	0.953

model. Furthermore, the higher LIK and the lower AIC and SC means that spatial lag model was more suitable than OLS model in exploring the relationship between variables. In addition, compared with OLS model, spatial lag model decreased the estimated regression coefficient of LOI, grain particle percent, and distance to Nanfei River mouth (Table 7). This is consistent with previous studies, i.e. if the spatial autocorrelation of environmental variables was accounted for, a part of the prediction would be based on the autoregressive term (Overmars et al. 2003). Meanwhile, the spatial lag parameter (ρ) is strong and significant, indicating the influence of Pb concentrations in sediments at nearby locations.

In the spatial lag model, the influence of grain particle percent on Pb concentrations is significant. This agrees with grain size effects, i.e. as sediment becomes finer, its surface specific surface area tends to be higher, and thus concentrations of metals increase. Therefore, when identifying hotspots, it is necessary to reduce grain size effects (in this study, EF values were employed to instead metal concentrations). In addition, it should be noted that when compared with OLS model, the significance of the grain particle percent in spatial lag model increased (Table 7), consistent with previous studies, i.e. when spatial autocorrelation was not taken into account, the biased significance would be obtained (Overmars et al. 2003).

When Liu & Shen (2014) studied metal concentrations in surface sediments of Chaohu Lake, they considered that the variations of low LOI values have less influence on metal concentrations. As per Table 7, spatial lag model revealed that LOI showed significant influence on Pb concentrations, inconsistent with their conclusion. Furthermore, previous studies have found that natural organic matter has a high affinity for metals in the aquatic environment (Fang et al. 2009). Therefore, in the study about the relationship between sediment properties and metal concentrations, organic matter content should be considered.

Huang et al. (2007) found that heavy metal concentrations in river sediments decreased as the distance away from the dominant source increase. Furthermore, Yin et al. (2011) also found that there was an overall tendency for metal concentrations to increase from estuarine areas of Nanfei River to the lake center. Similarly, in spatial lag model, the distance to Nanfei River mouth had a significant influence on variations of Pb concentrations (Table 7). Nanfei River is the most polluted river among the inflow rivers of west Chaohu Lake, and the EF of Pb at Nanfei River mouth was far higher than other river mouths. So, Nanfei River should be focused for pollution control and remediation.

CONCLUSIONS

In this study, 38 sediments and 4 river mouth sediments were analysed using local Moran's I, geostatistics and EF. LISA analysis revealed that Mn and Pb had high-high clusters, meaning there is some extent spatial enrichment of Mn and Pb in sediments. Furthermore, samples were classified according to pollution status and local spatial patterns, the results indicated that polluted samples are mostly in high-high clusters, while unpolluted samples generally belonged to low-low clusters. LISA map exhibited high-high clusters of Zn distributed in the north part of the study area, and high-high clusters of Mn in the central part of the study area. Geostatistic analysis showed that Co and Mn have high spatial dependence, and Pb weak spatial dependence. After analysis, Co is found to be mainly originated from natural sources, Mn is influenced by upward migration and reprecipitation, and Pb is influenced by anthropogenic sources.

The typical three metals showed obviously different characteristics. Sample distribution in local spatial patterns of Co, which is mainly from natural sources, is different from that of Mn and Pb that may be influenced by other sources. Furthermore, for metals influenced by other sources (Mn and Pb), the positions of hotspots, especially regional hotspots, may be different. Local Moran's I can be employed to not only effectively detect hotspots of metals, but also identify the pollution sources.

The relationship between heavy metal concentrations and environmental variables was analysed using SAR model and OLS model, and Pb was selected as an example. Compared with OLS model, SAR model has several advantages, including taking account of spatial autocorrelation, decrease of regression residuals, increase of LIK and pseudo R^2, and reduction of AIC and SC. In addition, grain particle percent and LOI were found to have significant influence on Pb concentrations, so in other similar studies, these should be taken into consideration. Furthermore, Nanfei River should be paid attention for pollution control and remediation of west Chaohu Lake. This is a new trial that explores the relationship between heavy metals and environmental variables from a spatial regression analysis perspective.

ACKNOWLEDGEMENT

This study was financially supported by the Fundamental

Table 7: OLS model and spatial lag model for Pb concentrations in sediments.

Model	Variable	Coefficient	t-stat	Probability
OLS model	Constant	5598.115	2.093	0.044
	LOI	5.855	10.943	0.000
	Grain particle percent	175.466	2.081	0.045
	Distance	-2.987	-3.465	0.001
	R^2 = 0.822, LIK = -133.210, AIC = 274.420, SC = 280.863, MIR = 0.148			
Spatial lag model	Constant	5562.187	2.394	0.017
	LOI	5.135	9.885	0.000
	Grain particle percent	174.795	2.387	0.017
	Distance	-2.713	-3.535	0.000
	ρ	0.275	2.674	0.007
	Pseudo-R^2 = 0.851, LIK = -130.200, AIC = 270.401, SC = 278.455, MIR = 0.009			

MIR: Moran's I of residuals.

Research Funds for the Central Universities, and the Research Funds of Renmin University of China (15XNL016).

REFERENCES

Anschutz, P., Dedieu, K., Desmazes, F. and Chaillou, G. 2005. Speciation, oxidation state, and reactivity of particulate manganese in marine sediments. Chemical Geology, 218(3-4): 265-279.

Chen, X., Yang, X.D., Dong, X.H. and Liu, Q. 2011. Nutrient dynamics linked to hydrological condition and anthropogenic nutrient loading in Chaohu Lake (southeast China). Hydrobiologia, 661(1): 223-234.

Dang, X. 1998. A review on Chao Lake area water environment. Environment Protection, 9: 38-39.

Dark, S.J. 2004. The biogeography of invasive alien plants in California: an application of GIS and spatial regression analysis. Diversity and Distributions, 10(1): 1-9.

Dassenakis, M., Andrianos, H., Depiazi, G., Konstantas, A., Karabela, M., Sakellari, A. and Scoullos, M. 2003. The use of various methods for the study of metal pollution in marine sediments, the case of Euvoikos Gulf, Greece. Applied Geochemistry, 18(6): 781-794.

Fang, T.H., Li, J.Y., Feng, H.M. and Chen, H.Y. 2009. Distribution and contamination of trace metals in surface sediments of the East China Sea. Marine Environmental Research, 68(4): 178-187.

Han, Y.M., Du, P.X., Cao, J.J. and Posmentier, E.S. 2006. Multivariate analysis of heavy metal contamination in urban dusts of Xi'an, Central China. Science of the Total Environment, 355(1-3): 176-186.

Hession, S.L. and Moore, N. 2011. A spatial regression analysis of the influence of topography on monthly rainfall in East Africa. International Journal of Climatology, 31(10): 1440-1456.

Hu, Y.N., Wang, D.X., Wei, L.J. and Song, B. 2014. Heavy metal contamination of urban topsoils in a typical region of Loess Plateau, China. Journal of Soils and Sediments, 14(5): 928-935.

Huang, B., Zhao, Y.F., Shi, X.Z., Yu, D.S., Zhao, Y.C., Sun, W.X., Wang, H.J. and Oborn, I. 2007. Source identification and spatial variability of nitrogen, phosphorus, and selected heavy metals in surface water and sediment in the riverine systems of a peri-urban interface. Journal of Environmental Science and Health, 42(3): 371-380.

Huo, X.N., Li, H., Sun, D.F., Zhou, L.D. and Li, B.G. 2012. Combining geostatistics with Moran's I analysis for mapping soil heavy metals in Beijing, China. International Journal of Environmental Research and Public Health, 9(3): 995-1017.

Huo, X.N., Zhang, W.W., Sun, D.F., Li, H., Zhou, L.D. and Li, B.G. 2011. Spatial pattern analysis of heavy metals in Beijing agricultural soils based on spatial autocorrelation statistics. International Journal of Environmental Research and Public Health, 8(6): 2074-2089.

Kissling, W.D. and Carl, G. 2008. Spatial autocorrelation and the selection of simultaneous autoregressive models. Global Ecology and Biogeography, 17(1): 59-71.

Li, G.L., Liu, G.J., Jiang, M.M., Wang, R.W. and Zheng, L.G. 2011. Partition characteristics and correlation of heavy metal between sediment and surface water from Chaohu Lake. Journal of University of Science and Technology of China, 41(1): 9-15.

Li, W.L., Xu, B.B., Song, Q.J., Liu, X.M., Xu, J.M. and Brookes, P.C. 2014. The identification of 'hotspots' of heavy metal pollution in soil-rice systems at a regional scale in eastern China. Science of the Total Environment, 472: 407-420.

Liu, E.F., Birch, G.F., Shen, J., Yuan, H.Z., Zhang, E.L. and Cao, Y.M. 2012a. Comprehensive evaluation of heavy metal contamination in surface and core sediments of Taihu Lake, the third largest freshwater lake in China. Environmental Earth Sciences, 67(1): 39-51.

Liu, E.F. and Shen, J. 2014. A comparative study of metal pollution and potential eco-risk in the sediment of Chaohu Lake (China) based on total concentration and chemical speciation. Environmental Science and Pollution Research, 21(12): 7285-7295.

Liu, E.F., Shen, J., Yang, X.D. and Zhang, E.L. 2012b. Spatial distribution and human contamination quantification of trace metals and phosphorus in the sediments of Chaohu Lake, a eutrophic shallow lake, China. Environmental Monitoring and Assessment, 184(4): 2105-2118.

Liu, G., Bi, R.T., Wang, S.J., Li, F.S. and Guo, G.L. 2013. The use of spatial autocorrelation analysis to identify PAHs pollution hotspots at an industrially contaminated site. Environmental Monitoring and Assessment, 185(11): 9549-9558.

Meyfroidt, P. and Lambin, E.F. 2008. The causes of the reforestation in Vietnam. Land Use Policy, 25(2): 182-197.

Overmars, K.P., de Koning, G.H.J. and Veldkamp, A. 2003. Spatial autocorrelation in multi-scale land use models. Ecological Modelling, 164(2-3): 257-270.

Rose, N.L., Boyle, J.F., Du, Y., Yi, C., Dai, X., Appleby, P.G., Bennion, H., Cai, S. and Yu, L. 2004. Sedimentary evidence for changes in the pollution status of Taihu in the Jiangsu region of eastern China. Journal of Paleolimnology, 32(1): 41-51.

Senesi, G.S., Baldassarre, G., Senesi, N. and Radina, B. 1999. Trace element inputs into soils by anthropogenic activities and implications for human health. Chemosphere, 39(2): 343-377.

Su, S.L., Jiang, Z.L., Zhang, Q. and Zhang, Y. 2011. Transformation of agricultural landscapes under rapid urbanization: A threat to sustainability in Hang-Jia-Hu region, China. Applied Geography, 31(2): 439-449.

Tang, R.L., Ma, K.M., Zhang, Y.X. and Mao, Q.Z. 2013. The spatial characteristics and pollution levels of metals in urban street dust of Beijing, China. Applied Geochemistry, 35: 88-98.

Wang, C., Liu, S.L., Zhao, Q.H., Deng, L. and Dong, S.K. 2012. Spatial variation and contamination assessment of heavy metals in sediments in the Manwan Reservoir, Lancang River. Ecotoxicology and Environmental Safety, 82: 32-39.

Wang, H. 2007. Spatial regression analysis on the variation of soil salinity in the Yellow River Delta. Proc. Spie., 6753(22): 67531-67539.

Wang, Y.Q., Yang, L.Y., Kong, L.H., Liu, E.F., Wang, L.F. and Zhu, J.R. 2015. Spatial distribution, ecological risk assessment and source identification for heavy metals in surface sediments from Dongping Lake, Shandong, East China. Catena, 125: 200-205.

Ye, X.Y. and Wu, L. 2011. Analyzing the dynamics of homicide patterns in Chicago: ESDA and spatial panel approaches. Applied Geography, 31(2): 800-807.

Yin, H.B., Deng, J.C., Shao, S.G., Gao, F., Gao, J.F. and Fan, C.X. 2011. Distribution characteristics and toxicity assessment of heavy metals in the sediments of Lake Chaohu, China. Environmental Monitoring and Assessment, 179(1-4): 431-442.

Yuan, G.L., Sun, T.H., Han, P., Li, J. and Lang, X.X. 2014. Source identification and ecological risk assessment of heavy metals in topsoil using environmental geochemical mapping: Typical urban renewal area in Beijing, China. Journal of Geochemical Exploration, 136: 40-47.

Yuan, H.M., Song, J.M., Li, X.G., Li, N. and Duan, L.Q. 2012. Distribution and contamination of heavy metals in surface sediments of the South Yellow Sea. Marine Pollution Bulletin, 64(10): 2151-2159.

Zhang, C.S., Luo, L., Xu, W.L. and Ledwith, V. 2008. Use of local Moran's I and GIS to identify pollution hotspots of Pb in urban soils of Galway, Ireland. Science of the Total Environment, 398(1-3): 212-221.

Zhang, T.T., Zeng, S.L., Gao, Y., Ouyang, Z.T., Li, B., Fang, C.M. and Zhao, B. 2011. Assessing impact of land uses on land salinization in the Yellow River Delta, China using an integrated and spatial statistical model. Land Use Policy, 28(4): 857-866.

Zhang, W.G., Feng, H., Chang, J.N., Qu, J.G., Xie, H.X. and Yu, L.Z. 2009. Heavy metal contamination in surface sediments of Yangtze River intertidal zone: An assessment from different indexes. Environmental Pollution, 157(5): 1533-1543.

Zheng, Z.X., Pan, C.R. and Ding, F. 2011. Distribution and environmental pollution assessment of heavy metals in surface sediments of Chaohu Lake, China. Journal of Agro-Environment Science, 30(1): 161-165.